
Article:
Zhang, Jie, Wang, Qiao, Mitchell, Paul Daniel orcid.org/0000-0003-0714-2581 et al. (1 more author) (2023) An Integrated Access and Backhaul Approach to Sustainable Dense Small Cell Network Planning. Information. 19. ISSN 2078-2489

https://doi.org/10.3390/info15010019

---

information

Article

An Integrated Access and Backhaul Approach to Sustainable Dense Small Cell Network Planning

Jie Zhang, Qiao Wang and Hamed Ahmadi *

School of Physics, Engineering and Technology, University of York, Heslington, York YO10 5DD, UK; jie.zhang@york.ac.uk (J.Z.); qiao.wang@york.ac.uk (Q.W.)
* Correspondence: hamed.ahmadi@york.ac.uk

Abstract: Integrated access and backhaul (IAB) networks offer transformative benefits, primarily their deployment flexibility in locations where fixed backhaul faces logistical or financial challenges. This flexibility is further enhanced by IAB's inherent ability for adaptive network expansion. However, existing IAB network planning models, which are grounded in the facility location problem and are predominantly addressed through linear programming, tend to neglect crucial geographical constraints. These constraints arise from the specific deployment constraints related to the positioning of IAB donors to the core network, and the geographic specificity required for IAB-node placements. These aspects expose an evident research void. To bridge this, our research introduces a geographically aware optimization methodology tailored for IAB deployments. In this paper, we detail strategies for both single-hop and multi-hop situations, concentrating on IAB donors distribution and geographical constraints. Uniquely in this study, we employ the inherent data rate limitations of network nodes to determine the maximum feasible hops, differing from traditional fixed maximum hop count methods. We devise two optimization schemes for single-hop and multi-hop settings and introduce a greedy algorithm to effectively address the non-convex multi-hop challenge. Extensive simulations across various conditions (such as diverse donor numbers and node separations) were undertaken, with the outcomes assessed against the benchmark of the single-hop scenario's optimal solution. Our findings reveal that the introduced algorithm delivers efficient performance for geographically constrained network planning.

Keywords: 60 GHz; mmWave; integrated access and backhaul; mix integer linear problem; location coverage problem; multi-hop; greedy algorithm

Citation: Zhang, J.; Wang, Q.; Ahmadi, H. An Integrated Access and Backhaul Approach to Sustainable Dense Small Cell Network Planning. *Information* **2024**, *15*, 19. https://doi.org/10.3390/info15010019

Academic Editor: Lin Chen

Received: 14 September 2023
Revised: 31 October 2023
Accepted: 22 December 2023
Published: 28 December 2023

1. Introduction

Integrated Access and Backhaul (IAB), an enhancement of long-term evolution (LTE) relay technology, was ushered in by the 3rd Generation Partnership Project (3GPP) in release-15 [1]. This innovation primarily addresses the challenges associated with the deployment costs of wired backhaul links and the extension of network coverage. In contrast to traditional base stations, IAB is operative in both the sub-6 GHz and the above 6 GHz spectrum [2]. It capitalizes on massive beamforming and the utilization of millimeter wave (mmWave), therefore facilitating the provision of backhaul with cost-effective bandwidth [3].

Figure 1 shows the architecture of an IAB network defined by 3GPP release-16 [4]. The network nodes in an IAB network are either IAB-donors or IAB nodes. The IAB donors connect to the core network with fiber and can provide wireless access services to mobile users as well as wireless backhaul to IAB nodes. The IAB nodes provide wireless access service to mobile users and wireless backhaul traffic to other IAB nodes as well. The IAB network introduces one or more wireless backhaul IAB nodes on the basis of the 5G New Radio (NR) network architecture, and the user equipment is able to access the network via intermediary nodes that facilitate extended connectivity. Furthermore, an IAB node

is designed to use the same basic infrastructure to provide wireless access and backhaul service for UEs and other IAB nodes, respectively, which means that the IAB nodes can be deployed densely and more flexibly. Therefore, these kinds of 'plug and play' design nodes are a more sustainable way of network planning to extend the coverage of the network. Since they avoid the need for large cabling and infrastructure intrusions, such as in road digging, their environmental footprint is greatly decreased. The durability and flexibility with which network designs may be updated to respond to increasing demands highlight the adaptability of IAB networks, ensuring that they remain a sustainable alternative for dynamic urban environments and changing connectivity needs.

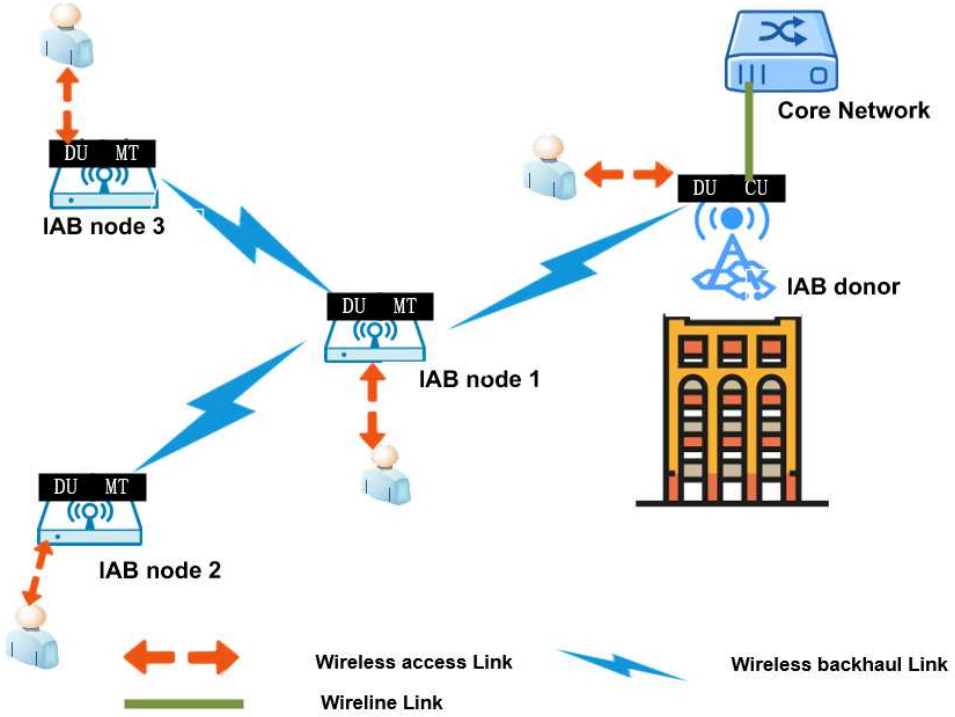

Figure 1. Integrated access and backhaul (IAB) architecture. The central unit (CU) in the IAB donor connects to the core network, while its distributed unit (DU) and the DU in the IAB nodes serve UEs and the other nodes. Mobile terminals (MTs) link with the DU of a parent node or donor.

In the realm of network planning, IAB networks have emerged as a pivotal strategy to enhance the density of mobile networks without the accompanying cost of fiber deployment. Within this ambit, ref. [5] showcases how using a standardized wireless technology for both access and backhaul (like the 5G New Radio standard) can offer flexibility in operation and compatibility across different IAB manufacturers. Their study highlights the merits of IAB, such as marked improvements in UE rates and its significance during incremental fiber deployments. While the authors present evidence for increased UE rates, they largely ignore the potential latency and spectrum shortage inherent in wireless backhaul. Taking a leap from there, ref. [6] highlights the ability of IAB networks to manage resources both centrally and distributively, proposing a coordinated parallel resource allocation scheme (CPReal) to seamlessly handle both bursty and non-bursty traffic. Exploring the technical details, ref. [7] investigates the challenges faced by full duplex-enabled IAB networks, especially concerning self-interference at millimeter wave (mmWave) frequencies. Although insightful, the study somewhat neglects the multifaceted interference sources and their cumulative impacts on network performance. In the quest for optimal deployment, ref. [8] highlights the importance of the densification of wireless networks and how mmWave small cells can aid in addressing increasing wireless demands, advocating for the adaptability of IAB networks in resource allocation. Ref. [9] proposed a

cell planning problem, emphasizing the trade-offs between deployment costs, SINR/rate coverage, and the versatility of algorithms like NSGA-II in tackling these challenges. The benefits of multi-hop backhauling over its single-hop counterpart are highlighted through optimizing association and resource allocation for IABs, as discussed by [10]. Ref. [11] illustrates the efficacy of resource allocation for mmWave multi-hop backhaul networks by modeling it as a matching game, while [12] stresses the challenges and strategies for network planning, specifically in the face of obstacle blockages in mmWave access networks. The authors of [13] introduce the complexities tied to the densification of the 5G RAN, emphasising the significance of effective backhaul planning for the small cell. The quandary between fiber-optic backhaul (which demands a higher CAPEX) and self-backhauled stations (leading to increased interference) further deepens the intricacies. The authors present a solution in the form of a GA-based hybrid backhauling technique, which offers superior performance in terms of the total cost of ownership (TCO) compared to wholly wired or unwired approaches. Concluding the analysis with [14], this paper highlights the issues associated with the placement of IAB nodes, especially in geographically constrained or interference-prone areas. By introducing mmWave blocking-aware constrained deployment optimization techniques, the paper establishes that despite the limitations inherent in deployment optimization, the diligent planning of networks can substantially enhance the coverage of IAB systems. Most of the studies referred to above, however, simplify and relax the requirements and practical constraints for where IAB nodes and donors are deployed in practice. The placement of IAB nodes and donors is typically chosen from a set of given potential locations that are deemed feasible based on various factors, including physical constraints, government regulations, and the optimization of network performance. Also, sufficient bandwidth needs to be provided for wireless backhaul.

Therefore, the motivation for this research emanates from the existing gaps in the current models of IAB network planning. High frequency mmwave bands increase the network's backhaul performance but introduce location and operational constraints due to significant pathloss and the necessity for precise IAB-node placements. Furthermore, the challenges are intensified as the IAB nodes must be selectively deployed from predefined potential locations, and the utilization of high-frequency mmWave necessitates stringent line of sight (LoS) conditions to mitigate the effects of pathloss. Traditional linear programming approaches with wireless backhaul, although effective, often overlook the intricate geographical constraints and the impacts of the significant mmWave pathloss. Our work aspires to solve these challenges by introducing an innovative, geographically aware optimization methodology that incorporates potential node locations, offering a comprehensive solution to the existing challenges in IAB deployments.

In this study, we address the challenges in IAB network planning, particularly in light of the location and number constraints necessitated by the IAB donors' wired connectivity to the core network. Recognizing the pivotal role of donor quantity and potential node locations, our research makes the following contributions:

- We use a mixed-integer linear programming (MILP) formulation to an architect-optimized single-hop network in scenarios characterized by a dense distribution of donors. This provides a robust framework to adeptly navigate IAB node deployment challenges.
- We formulate a non-convex multi-hop network problem in scenarios with sparse donor distribution. To overcome the inherent complexities of this formulation, we introduce a modified greedy algorithm, demonstrating its efficacy in the face of the non-trivial, NP-hard nature of multi-hop IAB deployments.
- We propose using the data rate constraint in our formulated one-hop and multi-hop problems, which departs from the traditional approach of limiting the hop length by a fixed number of hops. And a link budget analysis at 60 GHz is integrated to ensure the feasibility of achieving the specified data rate at the given frequency.

In essence, the developed methodologies and formulations are not exclusively confined to the realms of IAB but extend their applicability to a broader spectrum of network

planning scenarios involving mmWave and higher-frequency bands for wireless backhaul applications, especially under the stringent confines of limited potential node locations.

The remainder of this paper is organized as follows: In Section 2, we present a system model for IAB network planning. Section 3 presents the problem formulation for one-hop and multi-hop IAB network deployments with the introduction of the data rate constraint, and a greedy approach to solve the multi-hop problem. Simulation results are presented in Section 4, providing insight into minimizing IAB quantities while ensuring the access and backhaul services requirement during planning. Finally, Section 5 provides a brief conclusion.

2. System Model

We consider an IAB network consisting of IAB nodes and donors, operating in the 60 GHz license-exempt frequency band. The system is designed to achieve fiber-like data rates, reaching up to 1 Gbit/s. We specifically focus on a city-based deployment, incorporating a wireless mesh network, as illustrated in Figure 2.

Figure 2. A sample mmWave integrated access and backhaul (IAB) network model with directional antenna.

The candidate sites for IAB node deployment include urban infrastructures, such as lamp-posts and bus-stops. These locations are selected in a way to facilitate line-of-sight (LoS) transmission for user access whenever possible. Our design faces several challenges, particularly in identifying optimal installation locations for each of the IAB nodes while minimizing the total number of nodes. While potential multi-hop scenarios pose some limitations, this is further compounded by the need to ensure that the data transfer rates are consistently served.

To guide our discussion, we outline the following key assumptions governing the system model:

- **All nodes/donors are unified:** We introduce this assumption to streamline the network design and analytical processes. Each node and donor is characterized by a uniform access and backhaul radius. An area is considered covered if it lies within the access radius of a deployed node or donor. Similarly, a node is deemed serviceable by a donor if it is located within the donor's backhaul radius. This consistency and standardiation, together with the requirement that all nodes and donors are at the same height, eliminates deviations that may muddy network performance evaluations, allowing us to focus on optimising deployment sites.
- **LoS transmission is consistently maintained:** Operating in the 60 GHz band necessitates a focus on ensuring LoS connections, owing to the millimeter-wave (mmWave) characteristics, which are highly susceptible to blockages and attenuation. Consequently, the consistent maintenance of LoS transmissions is integral to attaining optimal data throughput and network performance. The nodes are, therefore, positioned to facilitate LoS, ensuring that the inherent propagation characteristics of the 60 GHz frequency are maximized to deliver robust connectivity.

To facilitate analysis, we assume that a certain number of donors pre-exist within an area, which is composed of one or more plane rectangular zones (an example is shown in Figure 3). Therefore, the core of our work is to deploy a finite number of nodes within potential locations to ensure that both access and backhaul requirements are adequately met.

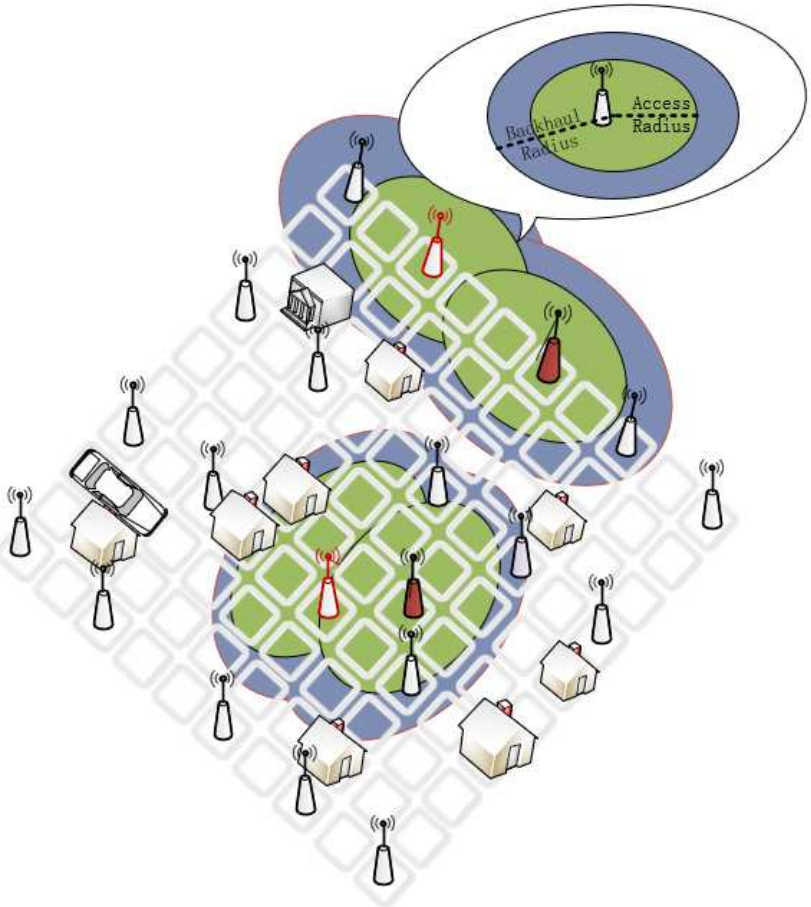

Figure 3. The grid indicates the area waiting to be covered and the location of deployment: solid red markers represent donors connected to the core network, red outlined markers denote deployed nodes, and white markers indicate potential node positions that remain undeployed. The green areas highlight the access coverage facilitated by the deployed nodes and donors, while the blue regions indicate the extent of backhaul coverage.

In our model, we aim to deploy IAB donors and nodes at designated candidate locations. Here, the candidate location of a node is symbolized as j, while i represents the exact coordinates where a donor is situated. Our primary objective is to determine the optimal deployment locations of the IAB nodes and, at the same time, to minimize the number of deployed nodes. We further define the communication model, ensuring that the power received at each grid center fulfills or surpasses a predefined signal-to-noise ratio (SNR) threshold, SNR_0. This requirement ensures that users (on the access side) are guaranteed to be provided with their necessary data rate service.

2.1. Communication Model

The foundation of our analysis revolves around understanding the received power, P_r, of a particular node. Mathematically, this can be described by the following [15]:

$$P_r = P_{node} + G_{all} - L_{all} - N_0, \tag{1}$$

$$G_{all} = G_t + G_r, \tag{2}$$

$$L_{all} = L_r + O_{tr} + L_{loss}, \tag{3}$$

$$N_0 = -174 + 10\log_{10}(W), \tag{4}$$

Here, P_r represents the received power in dB, while G_{all} signifies the cumulative antenna gains from the transmitting side G_t and the receiving side G_r. L_{all} embodies the total losses, which include the path loss L_{loss}, atmospheric attenuation O_{tr}, and rain-induced attenuation L_r, with N_0 denoting thermal noise.

Delving deeper into the path loss, it emerges as a function of the distance between nodes and encapsulates the consequences of signal propagation. Given the pronounced attenuation characteristics of 60 GHz mmWave, our parameter selections are crucial. We use the parameters 12.6 dB/km from ITU-R P.838 for rain attenuation if we consider an average annual rainfall rate of 35 mm/h [16]. To further strengthen our analysis, we also considered oxygen absorption of about 16 dB/km [17]. We undertook a comprehensive link budget analysis to ascertain the viability and performance of our proposed communication system and Figure 4 shows the results of the analysis.

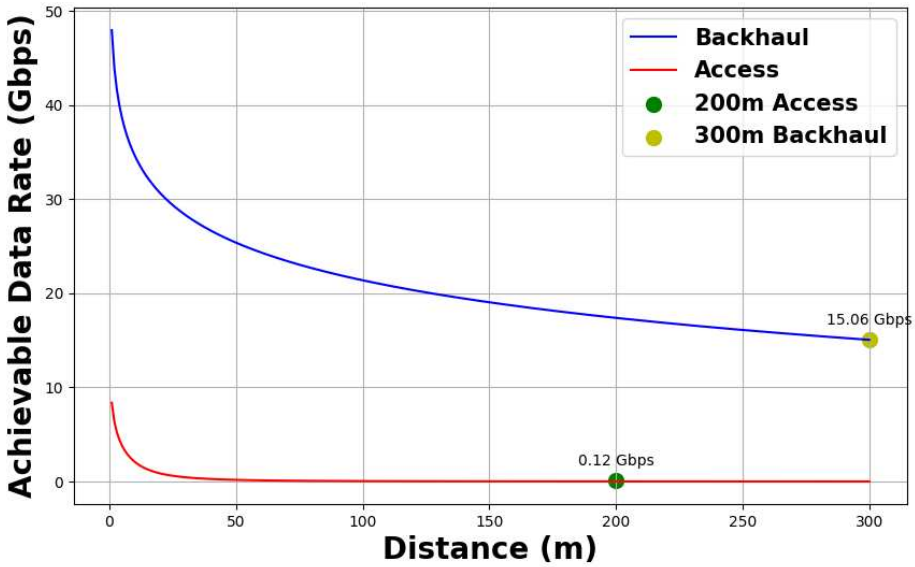

Figure 4. Achievable data rate for access and backhaul with transmit power 30 dbm, antenna gain for access side 5 dBi, directional antenna gain for backhaul side 30 dBi, and pathloss exponent 2.

Given the challenges posed by such pronounced path losses, the design aspiration for our system is heavily influenced by the advantages of antenna design. For the access

side, the preference is towards omni-directional antennas. Their innate ability to ensure consistent radiation across all horizontal trajectories is encapsulated by the gain expression:

$$G_{\text{omni}} = G_0, \tag{5}$$

where G_0 symbolizes the invariant gain regardless of direction.

On the flip side, backhaul links demand a more directional approach, specifically utilizing sector antennas. These are strategically chosen to counteract the challenges posed by atmospheric and rain attenuations. Their spatial filtering capabilities stand as a bulwark against interference, with the gain between two nodes expressed as:

$$G_{tr} = \begin{cases} G_t \cdot G_r & \text{if } \frac{-\theta_{HPBW}}{2} \leq \psi \leq \frac{\theta_{HPBW}}{2} \\ 0 & \text{otherwise} \end{cases} \tag{6}$$

We delineate our communication model with the distinct operational dynamics of access and backhaul links. The access link, characterized by connections between nodes/donors and user equipment, capitalizes on the ubiquitous coverage afforded by omni-directional antennas. In this domain, each node/donor produces a circular coverage footprint, ensuring extensive and uniform service delivery to user devices. In contrast, the backhaul link, tasked with establishing connections among nodes and between nodes and donors, employs fixed directional links. The employment of fixed directional links amplifies link reliability, curtails interference, and bolsters capacity. Therefore, we use circular representation for omni-directional coverage and use straight lines when considering backhaul links. Our primary goal remains to determine the minimum number of these conceptual circles required for full coverage. Such a modeling perspective finds its roots in prior scholarly research [18].

2.2. Data Rate Constraint

Figure 5 depicts a general K-hop IAB model. In this model, the link between two IAB nodes is the backhaul link, and the link between the node and the UE is the access link. Here, we only consider a typical backhaul link in a multi-hop IAB system where the source node α_k sends data to a destination donor through several relay nodes. In the analysis of communication network node performance, the management of data rates serves as a core metric. Specifically, the output data rate of each node must exceed its input data rate, due to "overhead", i.e., the additional data load in the communication process. This overhead may include a range of factors, such as error correction, protocol handling, and data encryption. In practice, this relationship ensures the robustness and reliability of the system while placing specific requirements on node design and the overall network architecture. It is important to emphasize that the overhead factor modifies the total outflow rate of the IAB contributing node to include any additional data processing or transmission tasks it undertakes. For general IAB nodes, the inflow rate is sourced from a preceding donor or another node dispensing backhaul services. The outflow from such a node includes both its local access needs and the backhaul obligations of any downstream nodes, assuming that it acts as a backhaul provider. Considering that as the number of hops increases, the data rate decreases until it is unable to serve the subsequent hops, we can formulate a network without the risk of loop by incorporating the data rate constraint.

An IAB node's (including both donor and relay nodes) outgoing data rate can be categorized into:

1. Its access rate from UEs.
2. The backhaul rate for succeeding nodes, considering that this IAB node provides them with backhaul services.

Consequently, the data rate relationship between each node and the next hop node can be mathematically represented as:

$$B_k = f(B_{k+1} + A_k) + C \tag{7}$$

In Equation (7), B_k represents the backhaul data rate at the k-th node. This rate is calculated as a function of both the backhaul data rate of the $k+1$-th node, denoted as B_{k+1}, and the access data rate at the k-th node, represented by A_k. The function $f(\cdot)$ denotes the application of a fixed overhead to the sum of B_{k+1} and A_k. C is a constant greater than 0.

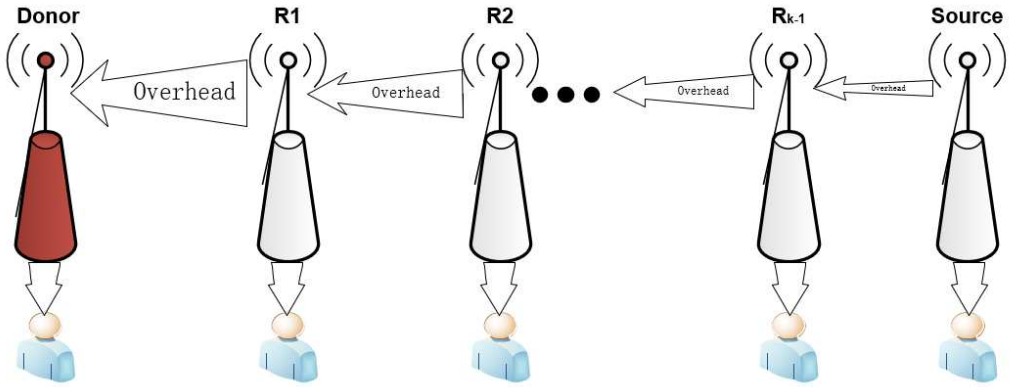

Figure 5. K-hop network's data rate constraint.

3. Problem Formulation

Given that the placement of IAB donors is predefined, which is mainly due to the availability of the fixed (optical) connections to the core network, our main objective is to minimise the number of nodes that need to be deployed while covering all the considered areas. This initiative lays the groundwork for broader network scalability. We first formulate and solve the problem for a one-hop scenario and then extend it to a multi-hop one.

Based on the presented system model, Figure 2 can be roughly translated into the two-dimensional map of Figure 3. We consider deploying IAB donors and nodes at candidate locations $j = (x_j, y_j) | \forall j \in J$ to provide coverage service. For simplicity, j represents the node's candidate location, while i denotes the location where a donor has been deployed. The grid to be covered is defined as $k = (x_k, y_k) | \forall k \in K$, ensuring that the power received at the grid center meets or exceeds the minimum SNR_0 requirement, thereby providing the necessary data rate service to users (access side).

3.1. One-Hop Problem Formulation

We define α_j as a binary indicator variable to show whether location i is selected to deploy a donor (1 for selected, 0 otherwise). Similarly, a binary variable α_j is defined to show node deployment in location j (1 for selected, 0 otherwise). $Y_{ij} \in \{0, 1\}$ is a backhaul service indicator when a donor deployed at i can provide the required backhaul service to a node placed at location j. Similarly, $C_{jk} \in \{0, 1\}$ and $C_{ik} \in \{0, 1\}$ are access service indicators when nodes placed at j and donors placed at i may serve k, respectively. The SNR is the basis for the indications of C_{ik}, C_{jk}. As the received power P_r is a function of distance, the required access/backhaul service is ensured when nodes/donors are positioned appropriately and P_r exceeds the threshold SNR_0.

3.1.1. Objective

The objective of the optimization problem is to minimize the number of nodes required to provide access and backhaul services whilst aiming to cover the whole area. As $\alpha_j = 1$ implies that a node will be deployed at location (x_j, y_j), the optimization goal is to minimize α_j:

$$\min \sum \alpha_j \tag{8}$$

3.1.2. Access and Backhaul Constraints

To determine the location of α_j, we consider a set of constraints grounded in both access service provision across the entire spatial region and one-hop wireless backhaul's data rate limitations. The following constraints elucidate the service provision mechanism:

- **Access Service Provision**: As defined by expression (9), there is a coverage constraint, meaning that the nodes should be deployed in a way to cover all the considered area. Expressions (10) and (11) further delineate the conditions under which a donor i and node j can collectively ensure coverage service to k, contingent on the SNR.

$$\sum_{i=1}^{I} a_i C_{ik} + \sum_{j=1}^{J} a_j C_{jk} \geq 1, \quad \forall k \in K \tag{9}$$

$$C_{ik} = \begin{cases} 1 & \text{if } SNR(d_{i,k}) > SNR_0 \\ 0 & \text{otherwise} \end{cases} \tag{10}$$

$$C_{jk} = \begin{cases} 1 & \text{if } SNR(d_{j,k}) > SNR_0 \\ 0 & \text{otherwise} \end{cases} \tag{11}$$

- **Backhaul Service Provision**: Expression (12) defines that each deployed node α_j must be supported by a donor i. Meanwhile, expression (13) ascertains that the donor's available data rate remains sufficient for service provision, even when catering for multiple nodes. This is premised on the assumption that the donor's capacity F_i is invariant, A_i solely depends on the donor's access data rate, and R_o is a fixed overhead. Hence, $\sum_{j \in J} Y_{ij} R_{ij}$ represents the data rate required for all nodes j connected to donor i:

$$\alpha_j - Y_{ij} \leq 0, \quad \forall i \in I, \quad \forall j \in J \tag{12}$$

$$F_i - R_o(A_i + (\sum_{j \in J} Y_{ij} R_j)) \geq 0, \quad \forall i \in I \tag{13}$$

- **Data Rate Interpretation**: The data rate R_{ij} between a donor at position i and a node at position j is formulated considering both the access data rate and the associated overhead:

$$R_{ij} \geq f(A_j) \tag{14}$$

where $f(x)$ is the linear function capturing the overhead and A_j is determined by the access data rate.

From the aforementioned analysis, it is evident that both the coverage and backhaul constraints must be satisfied while minimizing the number of nodes during the network planning process. Consequently, we present the optimization problem as follows:

$$\begin{gathered} \min \sum \alpha_j \\ \text{subject to:} \quad (9)(10)(11)(12)(13)(14) \\ C_7 : \alpha_j \in 1, 0, \forall j \in [J] \end{gathered}$$

All parameters are listed in Table 1. The formulated problem is a mixed-integer (binary) linear programming one which can be solved by solvers like CPLEX [19].

Table 1. One-hop and multi-hop formulation parameters.

One-hop and Multi-hop Formulation Parameters	
i	Pre-deployment donor location
j	Number of potential nodes locations
k	Number of grids needing to be covered
R_o	Overhead or required overhead
I	Set of all donor locations
J	Set of all potential nodes locations
K	Set of the locations on the grid that need to be covered
U	Set of the active users in the coverage of a donor or a node
α_j	Indicates whether the candidate location is chosen to deploy node
C_{ik}	Indicates whether grid $k \in K$ can be covered when node deployed at location $i \in I$
C_{jk}	Indicates whether grid $k \in K$ can be covered when node deployed at location $j \in J$
Y_{ij}	Indicates whether donor i can provide backhaul when node deploys in j or a donor deployed at $i \in I$ can provide backhaul to a node located at $j \in J$
Y'_{jn}	Indicates whether node at $j \in J$ can provide backhaul to the other node located at $n \in J$
Y'_{nm}	Indicates whether node at $n \in J$ can provide backhaul to the other node located at $m \in J$
d_{ij}/d_{pq}	Distance between two candidate nodes or two nodes p and q, where $p, q \in I \bigcup J \bigcup U$
R_{ij}/R_{pq}	Data rate between donor i and node j or between two nodes p and q, where $p, q \in I \bigcup J \bigcup U$
$A_i/A_j/A_x$	Access data rate when donor/node is deployed in i/j or access data rate of a node or a donor
F_i	Fixed data rate in of a donor $i \in I$

3.2. Multi-Hop Problem Formulation

The previous one-hop scenario makes it clear that it places strict requirements on the location and count of donor distributions. Recognizing that achieving a practical donor distribution is not always feasible, we propose a multi-hop problem model inspired by the single-hop problem scenario. The inherent multi-hop problem involves determining the most optimal node placement to ensure efficient data transfer via node-to-node communications whilst minimizing the number of nodes deployed.

3.2.1. Objective

The objective of this problem is to minimize the number of deployed nodes to cover all grid places:

$$\min \sum_{j \in J} \alpha_j \tag{15}$$

3.2.2. Coverage Constraint

Each grid place must be covered by at least one deployed node or one donor.

$$\sum_{j \in J} C_{jk} \alpha_j + \sum_{i \in I} C_{ik} \geq 1, \forall k \in K \tag{16}$$

3.2.3. Data Rate Constraint

For each deployed donor, the flow-in data rate should be a constant value determined by a fixed fiber data input rate. The data rate that flows out from a donor node comprises two parts: (i) the data rate required for its own access coverage, and (ii) the backhaul data rate required by the downstream nodes if the donor node provides backhaul service to them. It is important to note that the total flow-out data rate from a donor node is subject to an overhead multiplier, which accounts for any additional data processing and transmission overheads incurred in the donor node. For regular nodes, the flow-in data rate is contributed by the upstream donor or another node that provides backhaul service to them. The flow-out data rate from a regular node is constituted by its local coverage data rate requirements and the backhaul data rate for any downstream nodes, given the condition that this node provides a backhaul service to the next-hop node. Here, expression (17) describes the data rate limitation of the donor. Similar to the donor, the total data rate flow-out from a regular node is also multiplied by an overhead factor to account for additional data transmission overheads. It is also worth noting that a node will only function properly when it can secure a sufficient data rate service, or at least meet its own access consumption. Here, expression (17) describes the data rate limitation of a donor. Expressions (18) and (19) represent the data rate limitation of the node. The fundamental constraint in this optimization problem is that the total data rate flow-in for any node, whether it is a donor node or a regular node, must always exceed its data rate flow-out. This condition ensures the robustness and sustainability of the network's data rate distribution, allowing for uninterrupted data service across the network. Failure to meet this data rate condition would render the node inactive and disrupt the network deployment to the next hop:

$$F_i - R_o(A_i + (\sum_{j \in J} Y_{ij} R_{ij})) \geq 0 \quad \forall i \in I \tag{17}$$

$$R_{ij} Y_{ij} - R_o(A_j + \sum_{n \in J, n \neq j} Y'_{jn} R_{jn}) \geq 0 \quad \forall i \in I, \forall j \in J \tag{18}$$

$$R_{jn} Y'_{jn} - R_o(A_n + \sum_{m \in J, m \neq n} Y'_{nm} R_{nm}) \geq 0 \quad \forall j, n \in J \tag{19}$$

From the aforementioned analysis, it is evident that both access and backhaul constraints must be satisfied during the network deployment process. And the data rate constraint will automatically limit the number of the hops. Consequently, we present the optimization problem as follows:

$$\text{Minimize} \quad \sum_{j \in J} \alpha_j \tag{20}$$

$$\text{subject to:} \quad \sum_{i \in I} C_{ik} + \sum_{j \in J} C_{jk} \alpha_j \geq 1 \quad \forall k \in K \tag{21}$$

$$A_x = \sum_{u \in U} R_{xu} + C \quad \forall x \in I \bigcup J \tag{22}$$

$$0 \leq R_{pq} \leq SNR(d_{pq}) \tag{23}$$

$$(17)(18)(19) \tag{24}$$

$$Y_{ij} <= \alpha_j \tag{25}$$

$$Y'_{jn} < \alpha_j \tag{26}$$

$$\tag{27}$$

3.3. Greedy Approach to Multi-Hop Optimization Problems

The multi-hop problem formulated in the last section is characterized by its non-convex and mixed-integer nature and the non-convexity of the problem arising from the constraints involving products of decision variables (e.g., $R_{ij}Y_{ij}$), and the constraints involving a function of the SNR with respect to distance, which could be non-linear depending on the specific form of $f(x)$. Non-convex problems are generally more difficult to solve due to the potential existence of multiple local optimal solutions. This class of problems can be solved efficiently using heuristic or metaheuristic approaches [20]. It should be noted that the results of these methods are not guaranteed to be the optimal solutions but they will efficiently achieve good sub-optimums. To solve this complex problem, we consider using a greedy algorithm, an iterative algorithm that makes the locally optimal choice at each stage with the hope of finding the global optimum. The algorithm is divided into two stages: the coverage ttage (Algorithm 1) and the backhaul stage (Algorithm 2).

In the coverage stage, we aim to cover every grid. The network is initialized with the deployed donor only. The potential node locations are sorted by their capacity to cover uncovered grid points and iteratively added to the network if they are within the backhaul radius of a donor or another node in the network, resulting in updated covered grid points.

Algorithm 1: Coverage Stage

Input : Area: area needs to be covered, for example: 1000 m $*$ 1000 m
Potential_nodes: List of potential locations to deploy nodes
Network_nodes: List of initialized donor nodes and nodes to be decided
Coverage_radius: Radius for access coverage, for example: 200 m
Backhaul_radius: Radius for backhaul coverage, for example: 300 m

Output: Area: Updated covered areas
Potential_nodes: Updated list of potential nodes
Network_nodes: Updated list of network nodes

```
while there exist uncovered area do
    Filter potential_nodes within backhaul_radius of any donor in network_nodes;
    Sort the filtered potential nodes by their uncovered coverage potential;
    if filtered list is empty then
        break;
    else
        Add the highest potential node to network_nodes;
        Mark area covered by this node;
        Remove this node from potential_nodes;
    end
end
return Area, potential_nodes, network_nodes;
```

In the backhaul stage, the objective is to establish a coherent data flow topology. Taking into account the imperatives of reduced latency, augmented reliability, and enhanced throughput, a strategic inclination towards maximizing single-hop connections is promoted. This strategy facilitates a hierarchical structure where nodes, post their one-hop deployment, serve as anchor points for subsequent multi-hop connections, thereby ensuring comprehensive coverage, especially for nodes that lie beyond the donor's backhaul radius. Given the incorporation of directional antennas for the backhaul connections, interference is substantially minimized. Moreover, the rich spectrum afforded by mmWave technology provides the requisite bandwidth to accommodate a profusion of direct, one-hop connections. To methodically realize this network topology, we initiate a graph with the donor nodes as root vertices. Subsequently, deployed nodes are based on their proximity to the donor or the closest deployed node. Each node is then tethered to the nearest donor which fulfills the data rate prerequisites, thereby engendering a potential network linkage. Nodes

that are incompatible with these stringent constraints are relegated to a waiting list for subsequent analysis.

Algorithm 2: Backhaul Stage

Input : Area: area needs to be covered, for example: 1000 m $*$ 1000 m
Potential_nodes: List of potential nodes
Network_nodes: List of initialized network nodes
Backhaul_radius: Radius for backhaul coverage, for example: 300 m

Output: Grid: updated coverage area
Potential_nodes: Updated list of potential nodes
Network_nodes: Updated list of network nodes
Status: Boolean indicating if all nodes are connected

```
Identify non-donor nodes and store them in non-donor-list;
(First Hop: Connecting non-donor nodes to donor nodes)
foreach donor in Network_nodes do
    foreach node in non-donor-list do
        if node is within Backhaul_radius of donor and data rate constraints are satisfied
         then
            Connect the node to the donor forming a first-hop connection;
            Update backhaul data rates of donor and node;
        else
            if node is not yet in waiting_list then
                Add node to waiting_list;
            end
        end
    end
end
Multi Hop: Establish connections for nodes in the waiting list using nodes already
 connected in the first hop, to_connect_hops means all connected nodes, initial
 value is all first hop nodes.;
while waiting_list is not empty do
    Create an empty new_hops list;
    foreach other_node in to_connect_hops do
        foreach node in waiting_list do
            if node is within Backhaul_radius of other_node and meets data rate
             requirements then
                Establish a connection between node and other_node;
                Update their data rates;
                Add node to new_hops;
                Remove node from waiting_list;
            else
        end
    end
    if new_hops is empty then
        Break;
    end
    Update to_connect_hops with new_hops;
end
return Grid, Potential_nodes, Network_nodes, Status;
```

The algorithm persistently assesses the nodes within the waiting list, striving to bridge them to the most proximal node or donor that aligns with the data rate specifications. In the event that a compatible connection is unattainable, the specific node is extricated from

the network. This necessitates an update of the covered grid points, and consequentially, the algorithm reverts to the coverage stage to ensure that all grid points maintain their coverage integrity. The algorithm continues through these stages until all grid points are covered and all data rate constraints are satisfied, which indicates that a solution has been found. While the greedy algorithm does not guarantee to find the global optimum due to the non-convex nature of the problem, it is a practical choice for obtaining a feasible solution in a reasonable amount of time. Its performance can potentially be improved by incorporating additional strategies, such as local search or heuristics, depending on the specific characteristics of the problem at hand.

4. Simulation Result

4.1. Simulation Setup

The simulation is set in a 1000 $\times$ 1000 m grid, within which the potential nodes are systematically positioned every 10 m, echoing the real-world spacing of street lights and, thus, yielding 100 $\times$ 100 potential node sites. The donors, being the cornerstone of this simulation, are not predetermined but rather are introduced as variable elements. Their quantities and positions are randomly generated inputs, due to the in-the-real-world constraint of donors being tethered to the core network via wired connections. This introduces a level of unpredictability and variability into our simulations, ensuring that our model is not just theoretical but also works under various predefined donor cases. Based on the donor locations and number characterized by randomness, we proceed to incorporate statistical methods to analyse and comprehend the resultant effects on the algorithm's performance and efficacy. Each area within the 1000 $\times$ 1000 grid is mandated to be under the coverage of either a node or a donor. The nodes, in turn, are linked to the donors ensuring a seamless backhaul communication, underpinned by our assumption of line of sight (LoS) communication. This dual conditionality of coverage and backhaul ensures that the deployment of nodes is not just about coverage but is the requirement for effective communication back to the core network via the donors. In our simulation, to encapsulate the variation in data rates for different nodes or donors, each donor and node is assigned a random access data rate ranging from 0.1 Gbps to 1.5 Gbps (100 Mbps to 1500 Mbps). This diverse data rate ensures that our simulation delivers fiber-like access speed with random access. Also, each donor's capacity is at 15 Gbps, a specification that ensures the robustness and efficacy of the wireless backhaul communication. Also, the link budget analysis of Figure 4 ensures that such data rate assumptions are reasonable. An overhead of 1.2 is configured to account for various communication inefficiencies and to ensure a more realistic simulation scenario.

4.2. One-Hop Simulation Result

In the last section, we formulated the single-hop problem of IAB network planning for the random distribution of donors. To solve the formulated optimization problem, we adopted the Python-based Gurobi library, which has been shown to be efficient in previous location coverage problems [21].

Figure 6 is a testimonial to the simulation's effectiveness. With nine donors, randomly positioned, the simulation strategically orchestrated the deployment of a mere eight additional nodes to achieve full grid coverage.

To analyse the relationship between the number of donors and the number of feasible optimization models. We simultaneously monitor the accumulation of both feasible and infeasible optimization models until a total of 100 models is reached. In Figure 7, we illustrate the number of feasible models as the number of donors varies between 5 and 20. Feasible models representing the Gurobi optimizer can successfully find an optimal solution. The plot reveals a corresponding increase in the number of feasible models, highlighting the positive impact of the donor quantity on achieving practical solutions. As the number of donors increases, there is a greater likelihood of obtaining a feasible solution for the given coverage constraints and the number of donors required to cover

the area, leading to a reduction in the marginal benefits delivered as the donor density increases further.

The number of IAB nodes deployed when the number of donors increases from 5 to 20 is shown in Figure 8. The figure demonstrates a decline in the average nodes deployed as the quantity of donors escalates. The standard deviation around the mean indicates that the number of nodes deployed may be affected by factors including donor location. Furthermore, a deeper analysis of the results unveils a substantial increment in the total number of deployments, embodying both donors and nodes. Despite the surge in donors, the comprehensive number of deployments increases. This suggests that an increase in the number of donors does not necessarily deter the growth in the total deployments.

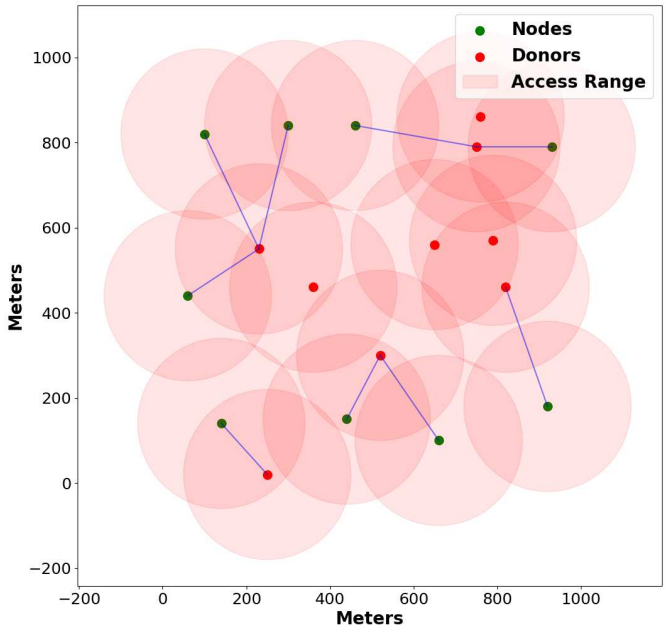

Figure 6. Optimization one-hop deployment result on a 1000 m ∗ 1000 m area with predefined donor positions, each donor/node's coverage radius is 200 m, and the backhaul radius is 300 m.

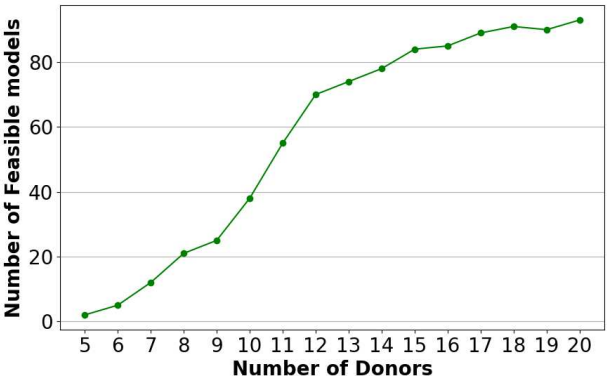

Figure 7. Number of feasible models of one-hop simulation for different numbers of donors.

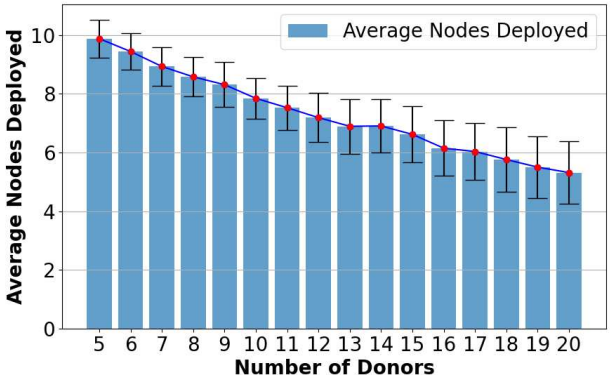

Figure 8. Average deployed nodes for one-hop optimal in 100 simulations with 200 m coverage radius and 300 m backhaul radius.

4.3. Multi-Hop Simulation Result

We formulated the multi-hop problem of IAB network planning for random sparse distributions of donors. In our pursuit to establish the effectiveness of the proposed algorithm, we initially embarked on a one-hop greedy simulation. The results obtained from the simulation were compared to the outcome of the earlier mixed-integer linear programming (MILP) optimization problem. As shown in Figure 9, we found that as the number of donors swells, the one-hop greedy algorithm becomes more proficient, gradually approximating the globally optimal solution provided by MILP. For example, when the donor count escalates to 20, this difference dwindles to approximately 0.5 nodes. This performance of the single-hop greedy algorithm, in particular the gradual agreement with the MILP results (less than one node difference) as the number of donors increases, is concrete proof of the effectiveness of the algorithm.

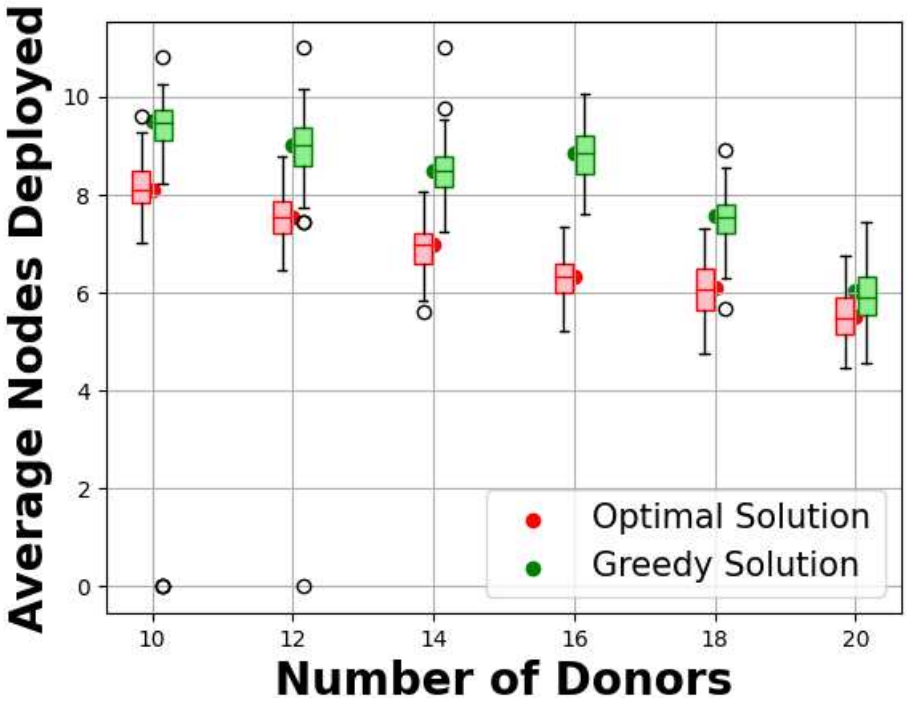

Figure 9. Comparison of average nodes deployed using one-hop optimal and one-hop greedy strategies as a function of the number of donors, with boxplots indicating variability around the means.

In the given multi-hop scenario, where the coverage radius and backhaul radius for each donor/node are stipulated at 200 and 300, respectively, a deployment comprising six donors resulted in the utilization of 16 nodes in one successful deployment, as shown in

Figure 10. One noteworthy observation from the results is that, while a node possesses the capability to connect with multiple donors, it does not necessarily imply simultaneous connections with all of them. Instead, this potential for multi-hop connections can be attributed to the donor providing sufficient data transfer rates to satisfy the node's requirements. This suggests that following a multi-hop formulation can effectively limit the hop length by the data rate constraint.

Next, we conducted a comparative analysis of the greedy multi-hop method and the one-hop optimal strategy. For each specified donor, we conducted 100 simulations and documented the results. There are significant differences between the one-hop optimal and the multi-hop greedy approach, as shown in Figure 11. Starting with only five donors, the one-hop yields two feasible models out of 100 simulations, compared to the multi-hop strategy's 12, which means that the multiple hops increase the likelihood of successful deployment. As donor nodes increase, the successful number for the multi-hop method grows more slowly than its optimal one-hop counterpart. At 11 donors, the one-hop method achieves 45 successful deployments, compared to the multi-hop's 62. And with the increment in donor nodes, the successful rates of both methods approach convergence, which means the advantage of the multi-hop strategy diminishes. Figure 12 investigates the influence of multi-hop on the average number of nodes deployed. The data reveal a trend of decrement in the average number of nodes concomitant with increment in the multi-hop. The values oscillate from an initial 16.916 with five donor nodes, attenuating to 7.914 when the donor nodes ascend to 20.

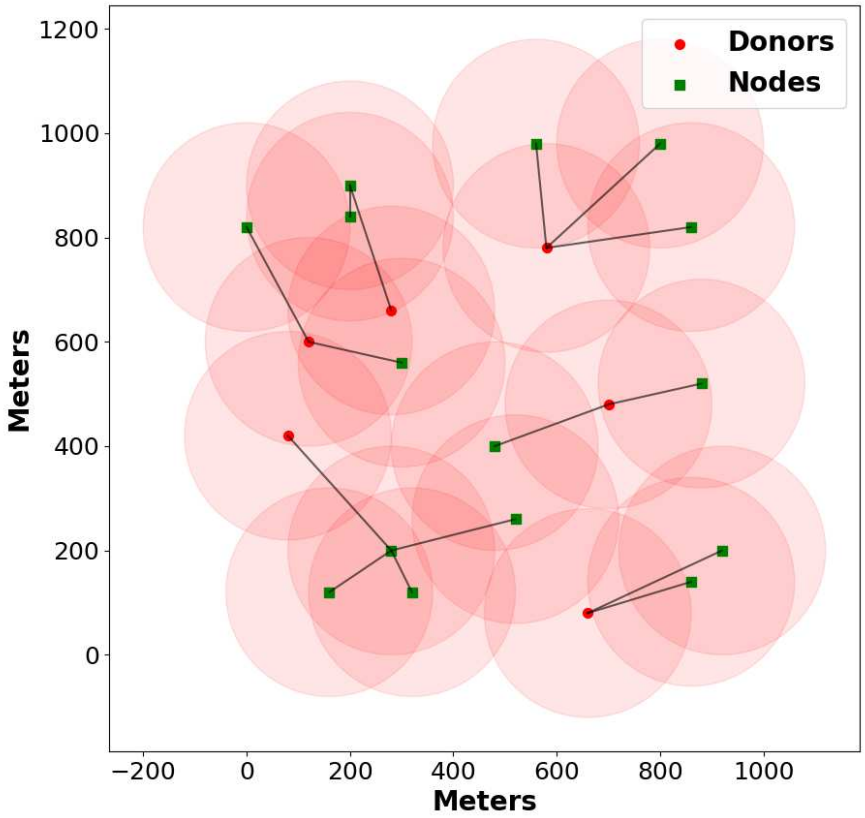

Figure 10. Deployment result of greedy multi-hop in a 1000 m ∗ 1000 m area with coverage radius 200 m and backhaul radius 300 m. The line shows that the remaining data rate of the current hop can provide enough backhaul service for the next hop.

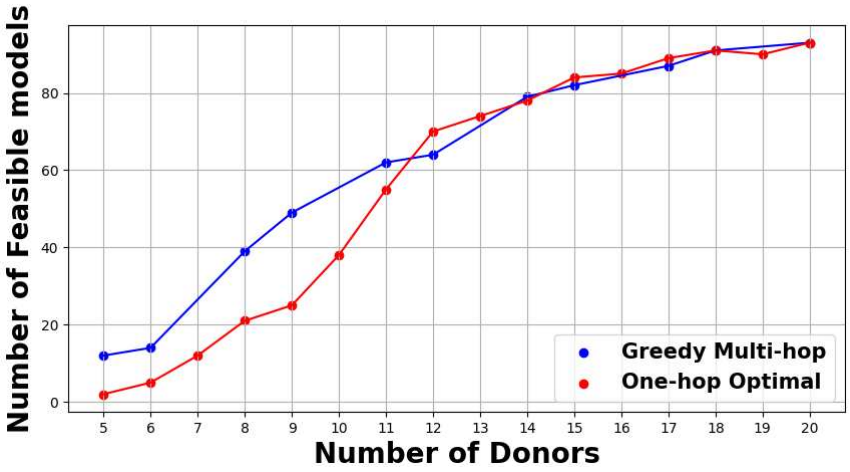

Figure 11. Number of feasible models out of 100 simulations between greedy multi-hop and one-hop optimal strategies across various donor counts.

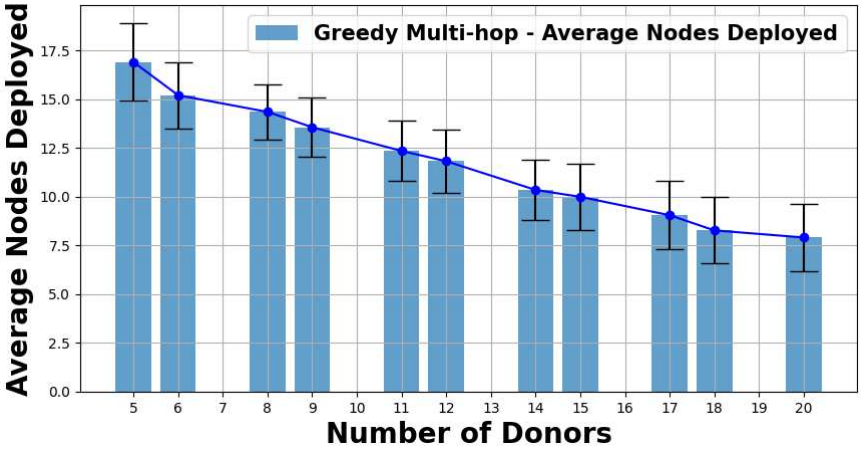

Figure 12. Average nodes deployed for the greedy multi-hop strategy with respective standard deviations across different donor counts

To examine the effect of the potential node location density on network coverage, we simulated various potential node distances ranging from 10 m to 50 m, with the results displayed in Figure 13. A critical observation from the early stages of network deployment emerged, particularly with fewer donors, such as five. The data suggest that as the gap between potential positions widens, the average number of nodes deployed incrementally increases. This implies that in environments with limited donors, larger separations might require deployment of more nodes for full coverage. Notably, in scenarios with five donors, choosing a separation of 10 m optimizes the deployment count, suggesting an efficient strategy for the initial stages. Conversely, in situations with a higher donor count, such as 20 donors, the influence of space on the node deployment diminishes, with values consistently ranging between 7.5 to 8.5, regardless of the separation distance.

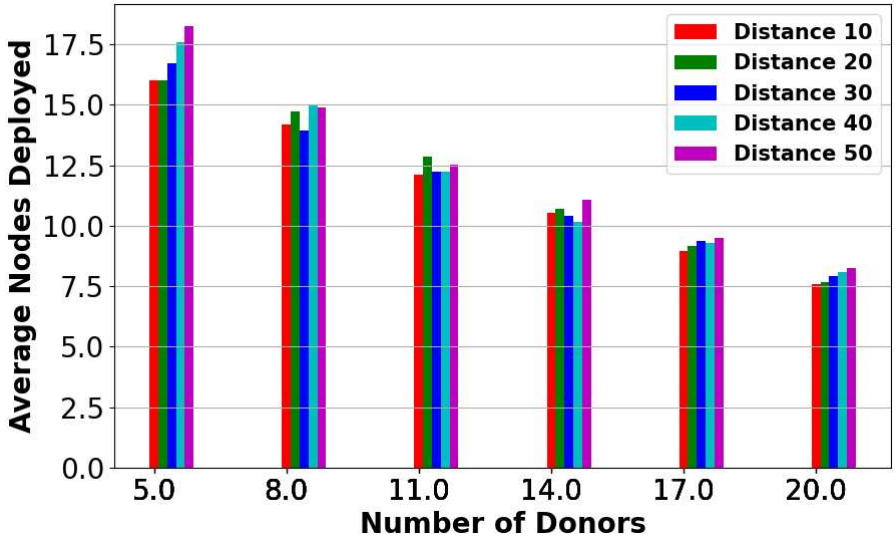

Figure 13. Comparison of average nodes deployed against the number of donors, differentiated by potential node distance from 10 m to 50 m. Potential node locations are distributed equidistant in a $1000 * 1000$ area and each distance showcases a distinct trend in node deployment as the donor count varies.

5. Conclusions

This paper provides insights into IAB network planning, imbued with a commitment to reducing the environmental impact and enhancing adaptability to a dynamic deployment strategy. Our approach capitalizes on the flexible deployment characteristic inherent to the IAB network, anchoring our optimization objective to minimize the number of node deployments. Our efforts have produced significant advancements, predominantly through the formulation and resolution of a single-hop network deployment strategy in the context of a dense donor distribution, which is directly responsive to the location challenges associated with IAB donors. We extended this progress to multi-hop scenarios for sparse donor environments, formulating an optimized network deployment strategy that caters for networks with arbitrary hop counts, while maintaining a keen focus on the geographical location of IAB donors. Challenging the conventional methodologies, we harness the intrinsic data rate constraints, which is substantiated by a link budget analysis, within donors to determine the maximum feasible hops, marking a departure from the practice of defining a rigid maximum hop count. This, in turn, offers a more nuanced and adaptive constraint to network length. The sustainable ethos, characterized by minimized environmental intrusion and enhanced adaptability to dynamic urban exigencies, underscores the relevance and applicability of our findings in contemporary and future network deployment scenarios. To solve the non-convex problem, we proposed a greedy algorithm, which effectively addresses the challenges associated with multi-hop network deployment. It is within this context that we showcase how IAB deployment is intricately influenced by geographical constraints, coverage constraints, and data rate considerations.

In conclusion, our study elevates the discourse on IAB network planning, offering nuanced insights and innovative methodologies that are attuned to the imperatives of sustainability, efficiency, and adaptability. Our contributions resonate with broader contexts of mmWave and higher-frequency bands deployments, particularly where the exigencies of location constraints are pronounced.

Author Contributions: Conceptualization, J.Z.; Methodology, J.Z.; Software, J.Z. and Q.W.; Validation, J.Z.; Formal analysis, J.Z.; Investigation, J.Z.; Resources, J.Z.; Writing—original draft, J.Z.; Writing—review & editing, J.Z., Q.W.; Visualization, J.Z.; Supervision, Q.W. and H.A.; Funding acquisition, H.A. All authors have read and agreed to the published version of the manuscript.

Funding: This research received no external funding.

Data Availability Statement: No new data were created or analyzed in this study. Data sharing is not applicable to this article.

Conflicts of Interest: The authors declare no conflict of interest.

Abbreviations

3GPP	3rd Generation Partnership Project
5G	the fifth generation of mobile networks
6G	sixth generation of mobile networks
ACO	Ant Colony Optimization
AI	Artificial Intelligence
AR	Augmented Reality
BB	Base Band
BBU	Base Band Unit
BCI	Brain Computer Interface
BER	Bit Error Rate
BS	Base Station
BW	bandwidth
C-RAN	Cloud Radio Access Networks
CAPEX	Capital Expenditure
CoMP	Coordinated Multipoint
CPU	Central Processing Unit
CR	Cognitive Radio
CRN	Cognitive Radio Network
D2D	Device-to-Device
DA	Digital Avatar
DAC	Digital-to-Analog Converter
DAS	Distributed Antenna Systems
DBA	Dynamic Bandwidth Allocation
DC	Duty Cycle
DL	Deep Learning
DRAM	Dynamic Random Access Memory
DRL	Deep Reinforcement Learning
DSA	Dynamic Spectrum Access
DT	Digital Twin
D-RAN	Distributed Radio Access Network
FBMC	Filterbank Multicarrier
FEC	Forward Error Correction
FFR	Fractional Frequency Reuse
FSO	Free Space Optics
GA	Genetic Algorithms
GPU	Graphic Processing Unit
HAP	High Altitude Platform
HL	Higher Layer
HARQ	Hybrid-Automatic Repeat Request
IoT	Internet of Things
IAB	Integrated Access and Backhaul
KPI	Key Performance Indicator
LAN	Local Area Network
LAP	Low Altitude Platform
LL	Lower Layer
LOS	Line of Sight

LTE Long Term Evolution
LTE-A Long Term Evolution Advanced
MAC Medium Access Control
MAP Medium Altitude Platform
MIMO Multiple Input Multiple Output
ML Machine Learning
MME Mobility Management Entity
mmWave millimeter Wave
MNO Mobile Network Operator
MR Mixed Reality
NASA National Aeronautics and Space Administration
NFP Network Flying Platform
NFPs Network Flying Platforms
NTNs Non-terrestrial networks
NFV Network Function Virtualisation
NN neural network
OAM Orbital Angular Momentum
O-RAN Open Radio Access Network
OFDM Orthogonal Frequency Division Multiplexing
OSA Opportunistic Spectrum Access
PAM Pulse Amplitude Modulation
PAPR Peak-to-Average Power Ratio
PGW Packet Gateway
PHY physical layer
PSO Particle Swarm Optimization
PT Physical Twin
PU Primary User
QAM Quadrature Amplitude Modulation
QoE Quality of Experience
QoS Quality of Service
QPSK Quadrature Phase Shift Keying
RF Radio Frequency
RL Reinforcement Learning
RN Remote Node
RRH Remote Radio Head
RRC Radio Resource Control
RRU Remote Radio Unit
RAN Radio Access Network
RIC RAN Intelligent Controller
SU Secondary User
SCBS Small Cell Base Station
SDN Software Defined Network
SNR Signal-to-Noise Ratio
SON Self-organising Network
TDD Time Division Duplex
TD-LTE Time Division LTE
TDM Time Division Multiplexing
TDMA Time Division Multiple Access
UE User Equipment
UAV Unmanned Aerial Vehicle
USRP Universal Software Radio Platform
VNF Virtual Network Function
vRAN Virtualized Radio Access Network
VR Virtual Reality
XAI Explainable Artificial Intelligence

References

1. 3rd Generation Partnership Project (3GPP). *Integrated Access and Backhaul for 3GPP Release 15*; Technical Specification or Technical Report DocumentNumberHere-if-Any; 3GPP: 2018. Available online: https://spectrum.ieee.org/3gpp-release-15-overview (accessed on 21 December 2023).
2. Alsaedi, W.K.; Ahmadi, H.; Khan, Z.; Grace, D. Spectrum Options and Allocations for 6G: A Regulatory and Standardization Review. *IEEE Open J. Commun. Soc.* **2023**, *4*, 1787–1812. [CrossRef]
3. Zhang, Y.; Kishk, M.A.; Alouini, M.S. A Survey on Integrated Access and Backhaul Networks. *Front. Commun. Netw.* **2021**, *2*, 647284. [CrossRef]
4. 3GPP. Integrated Access and Backhaul for 3GPP Release 16. Technical Report YourDocumentNumber, 3rd Generation Partnership Project (3GPP), 2020. Technical Specification (or Report). Available online: https://www.etsi.org/deliver/etsi_ts/138100_138199/138175/16.00.00_60/ts_138175v160000p.pdf (accessed on 21 December 2023).
5. Islam, M.N.; Abedini, N.; Hampel, G.; Subramanian, S.; Li, J. Investigation of performance in integrated access and backhaul networks. In Proceedings of the IEEE INFOCOM 2018—IEEE Conference on Computer Communications Workshops (INFOCOM WKSHPS), Honolulu, HI, USA, 15–19 April 2018; pp. 597–602. [CrossRef]
6. Yu, M.; Pi, Y.; Tang, A.; Wang, X. Coordinated parallel resource allocation for integrated access and backhaul networks. *Comput. Netw.* **2023**, *222*, 109533. [CrossRef]
7. Zhang, J.; Garg, N.; Holm, M.; Ratnarajah, T. Design of Full Duplex Millimeter-Wave Integrated Access and Backhaul Networks. *IEEE Wirel. Commun.* **2021**, *28*, 60–67. [CrossRef]
8. Islam, M.N.; Subramanian, S.; Sampath, A. Integrated Access Backhaul in Millimeter Wave Networks. In Proceedings of the 2017 IEEE Wireless Communications and Networking Conference (WCNC), San Francisco, CA, USA , 19–22 March 2017; pp. 1–6. [CrossRef]
9. Rezaabad, A.L.; Beyranvand, H.; Salehi, J.A.; Maier, M. Ultra-Dense 5G Small Cell Deployment for Fiber and Wireless Backhaul-Aware Infrastructures. *IEEE Trans. Veh. Technol.* **2018**, *67*, 12231–12243. [CrossRef]
10. Lim, B.; Lee, J.H.; Kwon, J.H.; Ko, Y.C. Joint Association and Resource Allocation for Multi-Hop Integrated Access and Backhaul (IAB) Network. *arXiv* **2021**, arXiv:cs.IT/2108.04483. [CrossRef]
11. Pu, W.; Li, X.; Yuan, J.; Yang, X. Traffic-Oriented Resource Allocation for mmWave Multi-Hop Backhaul Networks. *IEEE Commun. Lett.* **2018**, *22*, 2330–2333. [CrossRef]
12. Moro, E.; Filippini, I.; Capone, A.; Donno, D.D. Planning Mm-Wave Access Networks With Reconfigurable Intelligent Surfaces. *arXiv* **2021**, arXiv:cs.NI/2105.11755. [CrossRef]
13. Hore, A.; Paul, A.; Maitra, M. Cost-effective Policy for Deployment of Dense 5G RAN with Fiber and Wireless Backhaul Link. In Proceedings of the 2021 22nd Asia-Pacific Network Operations and Management Symposium (APNOMS), Tainan, Taiwan, 8–10 September 2021; pp. 142–147. [CrossRef]
14. Madapatha, C.; Makki, B.; Guo, H.; Svensson, T. Constrained Deployment Optimization in Integrated Access and Backhaul Networks. In Proceedings of the 2023 IEEE Wireless Communications and Networking Conference (WCNC), Glasgow, UK, 26–29 March 2023; pp. 1–6. [CrossRef]
15. Correia, L.; Frances, P. A propagation model for the estimation of the average received power in an outdoor environment in the millimetre waveband. In Proceedings of the Proceedings of IEEE Vehicular Technology Conference (VTC), Stockholm, Sweden, 8–10 June 1994; Volume 3, pp. 1785–1788. [CrossRef]
16. International Telecommunication Union-ITU . *ITU-R P.838: Specific Attenuation Model for Rain for Use in Prediction Methods*; Technical report; ITU Radiocommunication Sector: Geneva, Switzerland, 2003.
17. Siles, G.A.; Riera, J.M.; Garcia-del Pino, P. Atmospheric Attenuation in Wireless Communication Systems at Millimeter and THz Frequencies [Wireless Corner]. *IEEE Antennas Propag. Mag.* **2015**, *57*, 48–61. [CrossRef]
18. Fang, Y.; Brown, D. Base Station Deployment Optimization in Federated Networks with Multi-Hop Communication. In Proceedings of the MILCOM 2022—2022 IEEE Military Communications Conference (MILCOM), Rockville, MD, USA, 28 November–2 December 2022; pp. 1030–1037. [CrossRef]
19. Ahmadi, H.; Chew, Y. Evolutionary algorithms for orthogonal frequency division multiplexing-based dynamic spectrum access systems. *Comput. Netw.* **2012**, *56*, 3206–3218. [CrossRef]
20. Ahmadi, H.; Chew, Y.H.; Chai, C.C. Multicell multiuser OFDMA dynamic resource allocation using ant colony optimization. In Proceedings of the 2011 IEEE 73rd Vehicular Technology Conference (VTC Spring), Budapest, Hungary, 15–18 May 2011; pp. 1–5.
21. Anjinappa, C.K.; Erden, F.; Güvenç, I. Base Station and Passive Reflectors Placement for Urban mmWave Networks. *IEEE Trans. Veh. Technol.* **2021**, *70*, 3525–3539. [CrossRef]